

Optimized Photocatalytic Degradation of 4-Nitrophenol over N,S-codoped ZnO Photocatalyst

A. M. Usman¹

¹Department of Chemistry,
Federal College of Education (Technical) Bichi,
Kano, Nigeria

A. Dahiru²

²Department of Veterinary Physiology and Biochemistry,
Usmanu Danfodiyo University,
Sokoto, Nigeria

Abstract:- In this study, a well defined photoactive N,S-codoped ZnO catalyst was synthesized through by a low-temperature alkali co-precipitation of zinc acetate dihydrate precursor in presence of ammonium sulfate as dopants' source. The catalyst was characterized by X-ray diffraction (XRD), scanning electronmicroscopy (SEM), energy dispersive x-ray (EDX), UV-visible analysis and FT-IR spectroscopy. The diffraction peaks of undoped and N,S-codoped lines materials are in accordance with the wurtzite hexagonal phase of ZnO. The insertion of the dopants (S and N) and the vigorous agitation during the catalyst preparation caused a decrease in the crystallites size. Visible light photocatalytic studies were carried out using 4-nitrophenol (4-NP) as pollutant. The effect of experimental variables for the photocatalytic degradation such as pH, initial 4-NP concentration, temperature and catalyst loading was optimized based on central composite design (CCD) and response surface methodology. The results indicated that photocatalytic activity of N,S-codoped ZnO (99.3%) was better than undoped ZnO (82%), because the band gap of doped was lower than undoped ZnO photocatalyst which is herein attributed to shift in the band gap caused by the dopants.

Keywords: Photocatalyst, Irradiation, Semiconductor, Degradation, 4-Nitrophenol and N,S-codoped ZnO.

I. INTRODUCTION

The presence of toxic organic compounds such as phenol in storm and waste water effluent is reported to be a major impediment to the widespread acceptance of continuous water and environmental purification [5,6]. Phenols and their derivatives are well known for their bio-recalcitrant and acute toxicity. Phenols are being introduced continuously into the aquatic environment through various anthropogenic inputs. 4-nitrophenol as one of the phenolic compound, has a nitro group at the opposite position of the hydroxyl group on the benzene ring (UNEP, 2002). It irritates the eyes, skin, and respiratory tract. It may also cause inflammation of those parts. It has a delayed interaction with blood and forms methaemoglobin which is responsible for methemoglobinemia, potentially causing cyanosis, confusion, and unconsciousness. When ingested, it causes abdominal pain and vomiting. Prolonged contact with skin may cause allergic response. The LD₅₀ in mice is 282 mg/kg and in rats is 202 mg/kg (HSDB, 2016).

Nonetheless, 4-Nitrophenol (4-NP) is used for the synthesis of medicines, dye, explosives, leather coloring agents, and it is generated during the formulation of pesticides or photodegradation of pesticides that contain the nitrophenol moiety. Consequently, 4-NP occurs widely in industrial and agricultural wastewater, rivers and soils. The presence of substituent groups, e.g., nitro groups, on phenols increases the toxic effects on ecosystem and human health due to their persistence in the environment. Therefore, 4-NP was notified as priority organic pollutants by the United States Environmental Protection Agency, (USEPA, 2008).

The removal of this important pollutant from aqueous environment has been demonstrated by traditional methods such as adsorption [3], biodegradation [4] as well as advanced oxidation process [5]. The superiority of photocatalysis as an advanced oxidation process for the decontamination of organic pollutants cannot be overemphasized. In photocatalysis, band gap excitation is caused by suitable and sufficient irradiation, which results in the generation of electron-hole pairs. The hole is exceptionally strongly oxidizing, thus allowing the generation of secondary oxidizing species (such as hydroxyl radical), which together can cause the degradative oxidation of organic pollutant.

In the photocatalytic removal of organic contaminants, a growing interest towards zinc oxide (ZnO) has arisen, due to its broad range of properties such as environmentally friendly, chemical stability, highly reactive and cost effective photocatalyst [6,7]. However, the efficiency of ZnO is partly limited by its rapid recombination of electron and hole [8], in addition to its incapacity to span the visible range of electromagnetic spectrum. Among the many attempts made to drastically reduce electron-hole recombination, doping plays a central role [9]. Previous workers showed inappreciable enhancement in the photocatalytic degradation of methyl orange [10] and 4-nitrophenol [11] by metallic doping of ZnO. The potential of nonmetal-doped photocatalysts is appealing because of the ability of such non-metal like nitrogen and sulphur to reduce the band gap energy required for excitation and enhance photoactivity [11]. In this work, C,N and S-codoped ZnO was synthesized by co-precipitation method and utilised in the photocatalytic removal of 4-nitrophenol, a model phenol derivatives under visible light irradiation.

II. EXPERIMENTAL PROCEDURE

➤ Chemicals

All the chemicals used in this experiment are of high analytical grade and include, Zinc acetate dihydrate (99%) Kernel product, Ammonium sulphate (99.5%) Aldrich product NaOH (98%, Sigma), 4-nitrophenol (product of merck), HCl(97% Sigma), as well as other chemicals, were used in the synthesis of catalyst as received. Deionized distilled water was used in the preparation of 4-nitrophenol and other reagents as used in this research.

➤ Synthesis of N,S-codoped ZnO

All reagents were used directly without further modification. The N,S-codoped ZnO was prepared through co-precipitation method. Zinc acetate dihydrate $Zn(CH_3COO)_2 \cdot 2H_2O$ was used as the precursor for ZnO and ammonium sulphate $(NH_4)_2SO_4$ as source of N and S, ethanol was used as reducing agent and sodium hydroxide as precipitating agent. In a typical procedure, 100ml of ethanol was added into 250ml zinc acetate solution (1M) and stirred for 5minutes, was then transferred in to an empty 1000ml beaker. Another 100ml of ethanol was added to 250ml of ammonium sulphate solution (M) in a separate beaker and stirred for 5minutes, and then transferred into the 1000ml beaker containing the zinc acetate/alcohol mixture. The heterogeneous mixture of $Zn(CH_3COO)_2$ /ethanol and $(NH_4)_2SO_4$ /ethanol in the 1000ml beaker was then subjected to vigorous stirring with the aid of magnetic stirrer for 30minutes for proper mixing. The mixture was then heated to 50°C and precipitated by the addition of 0.1M NaOH solution under stirring until the pH of the mixture was 7, then maintaining the temperature at 50°C and vigorous stirring for 2hours using the magnetic stirrer. The resulting mixture was then removed out of the heating source containing the stirring, and allowed to cooled down for 4hours. A white precipitate settled down, leaving the clear liquid at the upper layer. The clear liquid was run off, leaving the white substance at the bottom of the beaker. This followed by centrifugation at 3000rev/minutes for 15minutes, and the white precipitate was obtained. The precipitate was washed three times with distilled deionized water, and then with ethanol to removed any traces of unwanted elements or ions that may be present in the mixture. It was then transferred to crucibles and taken in to oven and dried at 60°C for 12hours. It was followed by calcinations at 450°C for two hours at the rate of 5°C/minute in a furnace, it was then allowed to cooled down, grounded using agate mortar and pestle, the resulting substance is a dark whitish powdered substance, was labeled as N,S-codoped ZnO.

Similar procedure was followed in preparation of the undoped ZnO, but ammonium sulphate was not used here (dopants not needed), the precipitation was done without heating, and was subjected to continuous and vigorous stirring for 2hours. It was then allowed to settled for 1hour. A white precipitate settled down at the bottom, leaving the clear solution at the top. It was then separated by centrifugation at 3000rev/min for 15minutes, washed 3times with distilled de-ionized water and then with ethanol. It was

then dried at 60°C for 12hours. It was followed by calcinations at 450°C for two hours at the rate of 5°C/minute, and the resulting substance was allowed to cooled down, grounded using agate mortar and pestle, a whitish powdered substance was obtained, and labeled as undoped ZnO.

➤ Catalyst Characterization

The percentage composition of N (nitrogen) and S (sulphur) in the synthesized codoped catalysts and the surface morphology was determined through scanning electron microscopy (SEM) at accelerating voltage of 15kV and magnification of 2500 times using Phenom pro X energy dispersive x-ray fluorescence spectrometer. The crystallinity and phase purity of the synthesized catalysts were analyzed using a ARL X, TRA diffractometer having Ni-filtered $Cu K\alpha$ radiation ($\lambda = 0.0154$ nm, 30 kV and 30 mA). The XRD patterns of the powders were recorded in the 2θ range of 2-70°. The scan rate was 2°min^{-1} . The particle size data was analyzed using Fullprof suite March 2017 based free software version. In order to determine the band gap energy of the catalysts, diffuse reflectance data were recorded on Perkin-Elmer Lambda 35 UV-Vis-NIR spectrophotometer. The reflectance data was related to the energy absorbed using the Schuster-Kubelka-Munk remission function.

➤ Photocatalytic Studies

In a specific experiment, 0.2g of calcined sample of N,S-codoped ZnO powder was dispersed in 100ml of 4-nitrophenol solution having a concentration 4Mg/L and pH of 7. The above suspension was stirred for 30min in the dark to obtain adsorption-desorption equilibrium to eliminate the error due to any initial adsorption effect. Then this was irradiated in a glass photo reactor of 385nm using 500W high-pressure Hg lamp of intensity 0.0129W/m^2 . Degradation was monitored by taking 5ml aliquots at different intervals of time. These aliquots were centrifuged for 15 min at 2000rev/min prior to absorbance measurements in order to eliminate the error due to scattering. Changes in the concentration of 4-nitrophenol (4-NP) are observed from its characteristic absorption at 316 nm. The concentration of 4-NP was determined spectrophotometrically using a lamda 35 UV-Visible spectrometer (Perkin Elmer). The temperature reached during the irradiation was 30 ± 2 °C. After the absorbance measurement, The efficiency of 4-NP degradation \hat{Y}_{exp} was calculated as follows (Equation 1):

$$\text{Degradation efficiency}(\hat{Y}_{\text{exp}}, \%) = \frac{C_0 - C_t}{C_0} \times 100\% \quad (1)$$

where C_0 and C_t represent the initial concentration of pollutant and concentration of pollutant at time 100 minutes respectively.

➤ The Experimental Design

To find the optimum conditions of the photocatalytic degradation of 4-nitrophenol, the experiments were designed by RSM and a five-level, three-variable central composite design (CCD) was employed. The independent variables

considered are the initial concentration of 4-NP (A), mass of catalyst (B) and pH (C). As the CCD is rotatable, there are five level of these variables and five codes (-1.682, -1, 0, +1, +1.682). These coded levels are displayed in Table 1. Other variables such as agitation speed, light intensity, oxygen

pressure and delivery volume were kept constant. The plan contained 8 factor points, 6 axial points and 6 center points. The total number of performed runs were 20 experiments as informed by formula $N(\text{experiments}) = 2^n + 2n + 6$, where n is the number of variables.

Table 1 Levels and Codes of Experimental Variable

Experimental Variables	Notation	Coded levels				
		Very Low	Low	Central	High	Very High
		(-α)	(-1)	(0)	(+1)	(α)
Initial 4-NP						
Concentration (mg/l)	A	1	2	6	10	15
Catalyst mass (g)	B	0.02	0.05	0.15	0.2	0.4
Initial pH	C	1.0	3.0	7.0	11	12

The degradation efficiency calculated using equation (1) is designated as the experimental response. Correspondingly, the experimental data can be processed using Design-Expert version 6.0.6 software to obtain predicted responses, response surfaces and regression model.

III. RESULTS AND DISCUSSIONS

➤ *Catalysts Characterization*

Powder X-rays diffraction (XRD) patterns were recorded with a *Thermo scientific* XRD machine of model *ARL X'' TRA with X-ray diffractometer*. The intensities were obtained in the 2θ ranges between 20° and 70°. The FULPROF software was used for estimating the average size of the crystallites. Rietveld refinement was performed on the diffraction patterns to determine the crystallite size and relative abundance of phases.

XRD patterns for the synthesized samples as shown in the Figure 1, The diffraction peaks of undoped Figure 1(a) lines and doped Figure 1(b) lines materials are attributable

to the (1 0 0), (0 0 2), (1 0 1), (1 0 2), (1 1 0), (1 0 3), (2 0 0), (1 1 2), and (2 0 1) planes which are in accordance with the wurtzite hexagonal phase of ZnO. These patterns are similar in both undoped and doped samples, assessing that neither the introduction of the dopants (N and S) nor the agitation during synthesis changes the crystal structure of ZnO.

The average crystallite sizes of particles were estimated by the Scherer's formula as shown below:

$$D = 0.89\lambda / \beta \cos\theta$$

Where D is the crystallite size, λ is the X-ray wavelength, β is the broadening of the diffraction peak and θ is the diffraction angle for maximum peak [12].

These values are 126 and 102 nm for C-doped ZnO and N,S-codoped ZnO samples respectively. The synthetic method employed shows that the insertion of dopants and the vigorous agitation caused a decrease in the crystallites size, i.e more dopants lead to decrease in crystallite size.

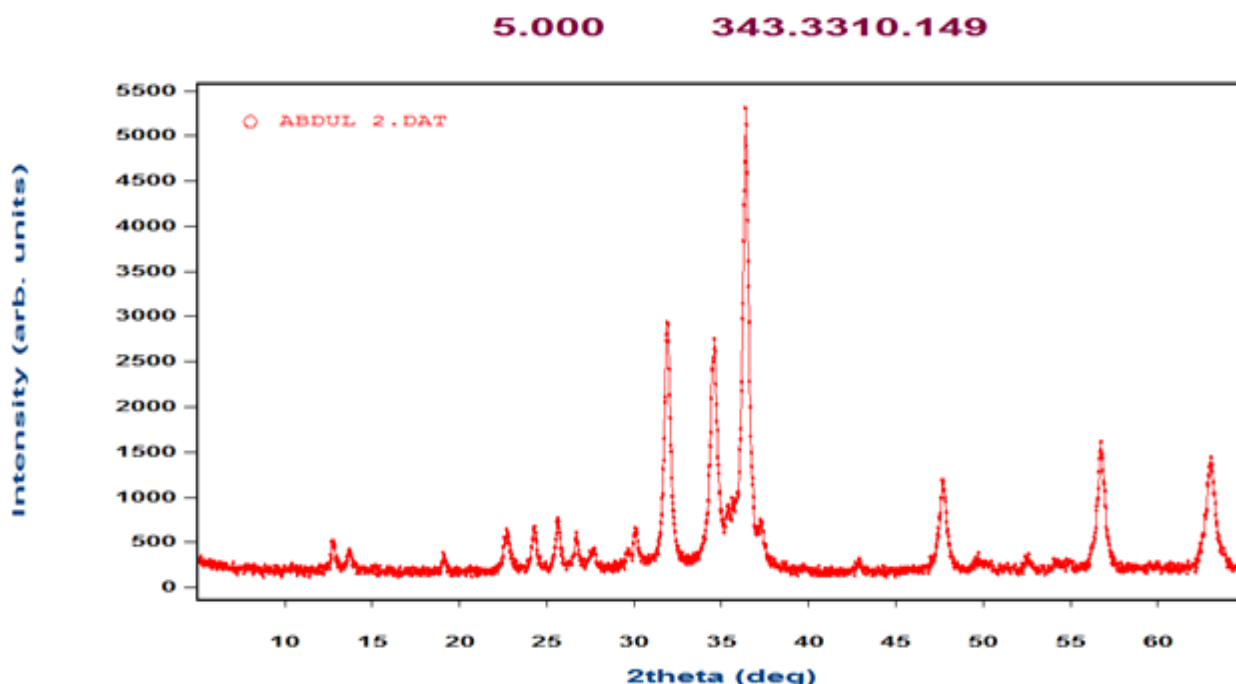


Fig 1 (a) XRD Patterns of Undoped ZnO

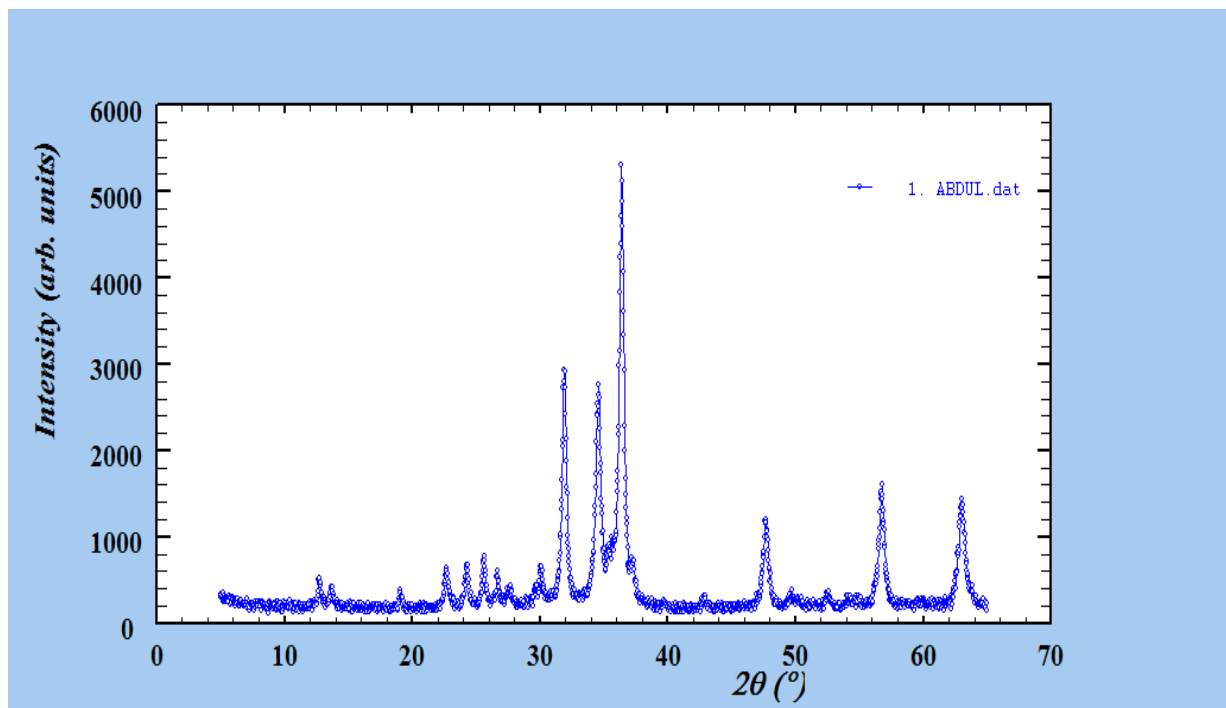


Fig 1 (b) XRD Patterns of N,S-co-doped ZnO

Table 2 Particles Size and Band Gap Energy of Undoped and N,S-codoped ZnO

Catalysts	Average particle size (nm)	Band gap energy (eV)
Undoped ZnO	126	3.28
N,S co-doped ZnO	102	3.05

The UV visible spectrum of the samples is as shown in figure 2 : The undoped ZnO absorbs the radiations in the UV range up to 365.14nm, while the N,S-codoped ZnO absorbs up to the range of 358nm, and almost all the visible spectrum radiations are transmitted by the ZnO nanoparticles.

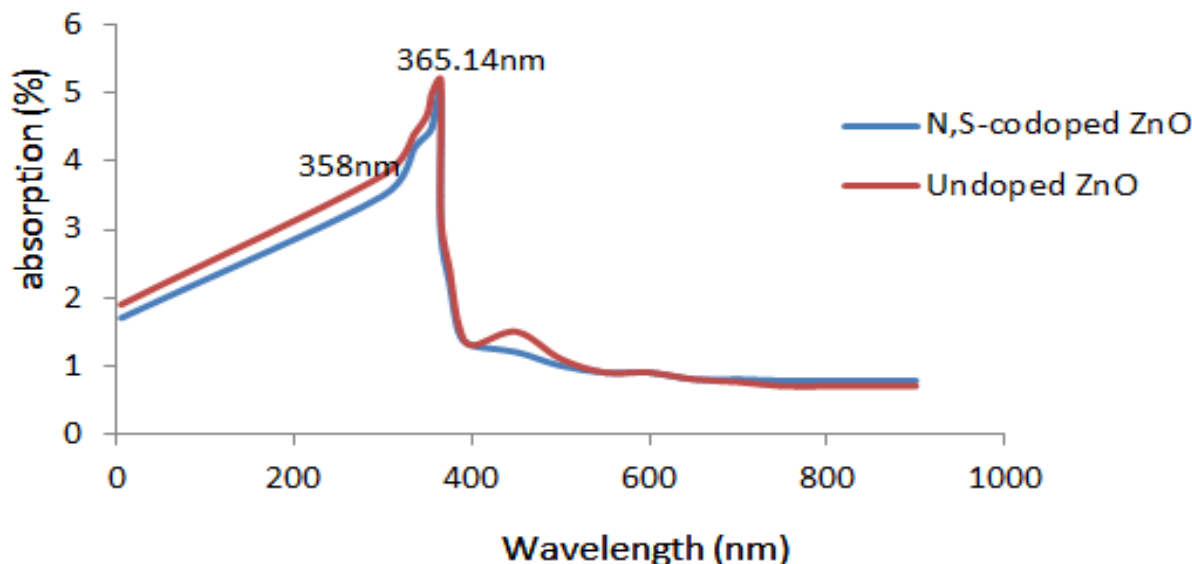


Fig 2 UV Visible Spectrum of Undoped and Doped ZnO

The band gap of the ZnO particles was calculated by extrapolating the curve drawn between $(h\nu)$ and $(\alpha h\nu)^{1/2}$ shown in figure 3. Where ν is the frequency and α is the optical absorption coefficient. The band gap energy obtained by extrapolating the curves was found to be 3.28 and 3.05eV for undoped and N,S-codoped ZnO eV respectively. This imply that the doping process has induced some small modification in the material band gap. This effect is one of the expected phenomenon for any semiconductor which undergo doping. The ordinates of the plot are basically the Schuster-Kubelka-Munk remission function $(F(R)h\nu)^{0.5}$ while the abscissae are the photon energies $(h\nu)$. The power 0.5 is the optical transition constant for ZnO, being an

indirect band gap semiconductor. From both the spectral plot and the table, red shift can be readily noticed. This may be due to an increase in the percentage of the dopants (N and S). This may be attributed to the introduction of new energy levels into the ZnO band gap as a result of the introduction of N and S, [13,17].

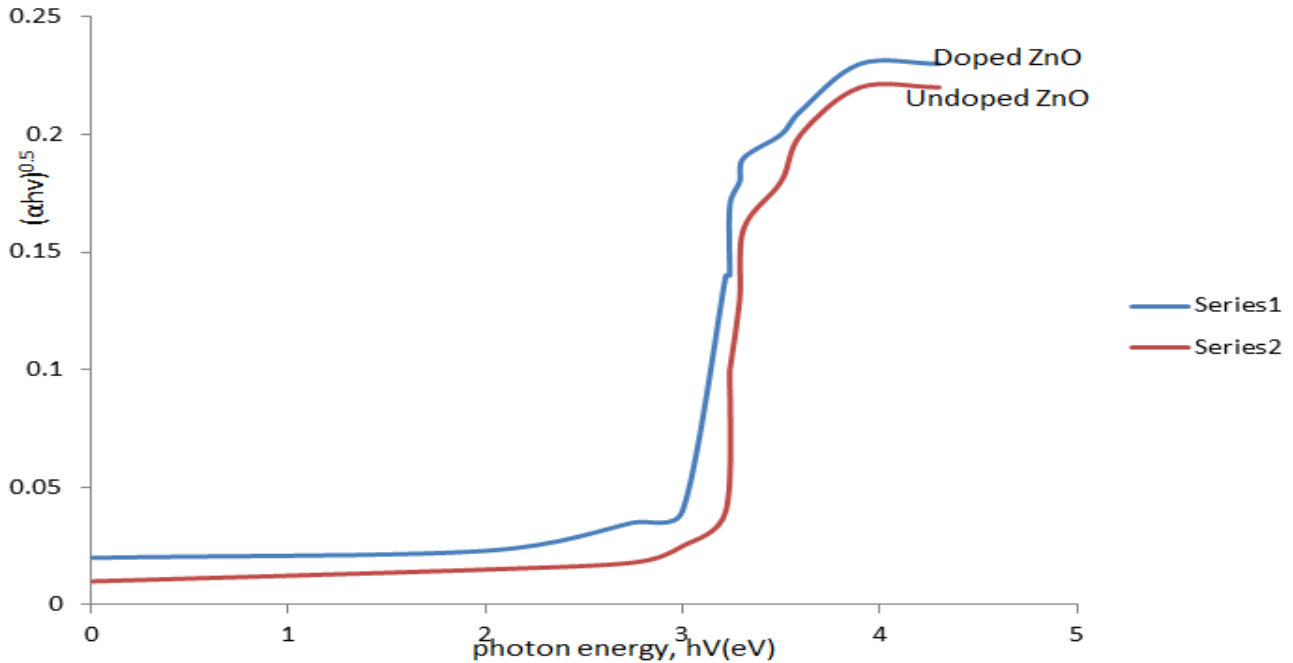


Fig 3 Extrapolation Curves of Undoped and N,S co-doped ZnO for Band Gap Determination

The figure 4 (a) and (b) shows the energy dispersive x-ray(EDX) spectra of undoped and N,S co-doped ZnO respectively. On the figure 4(a) , Zn appeared at 1keV with longest peak in the spectra while oxygen appeared at 0.5keV. Other impurity elements which are carbon and gold also appeared on the spectra. Gold comes probably from the SEM operator used in the analysis of the doped and undoped ZnO samples. The undoped sample contains 70.5% Zn and 13.4% oxygen, hence the sample synthesized is a 85% ZnO. The minute concentration of the impurity is insignificant to affect the photocatalytic activity of the ZnO.

Figure 4(b) is edx spectra of N,S co-doped ZnO. The Nitrogen atom appeared at 0.5keV while S appeared at about 2.4keV with the peak of sulphur appeared to be longer than that of nitrogen. This shows that the percentage of sulphur in ZnO is higher than that of nitrogen. The N and S codoped ZnO contains 83.9% ZnO, 5.4% sulphur and 1.9% nitrogen. This has justified the doping of nitrogen and sulphur in to the ZnO to produced N and S doped ZnO.

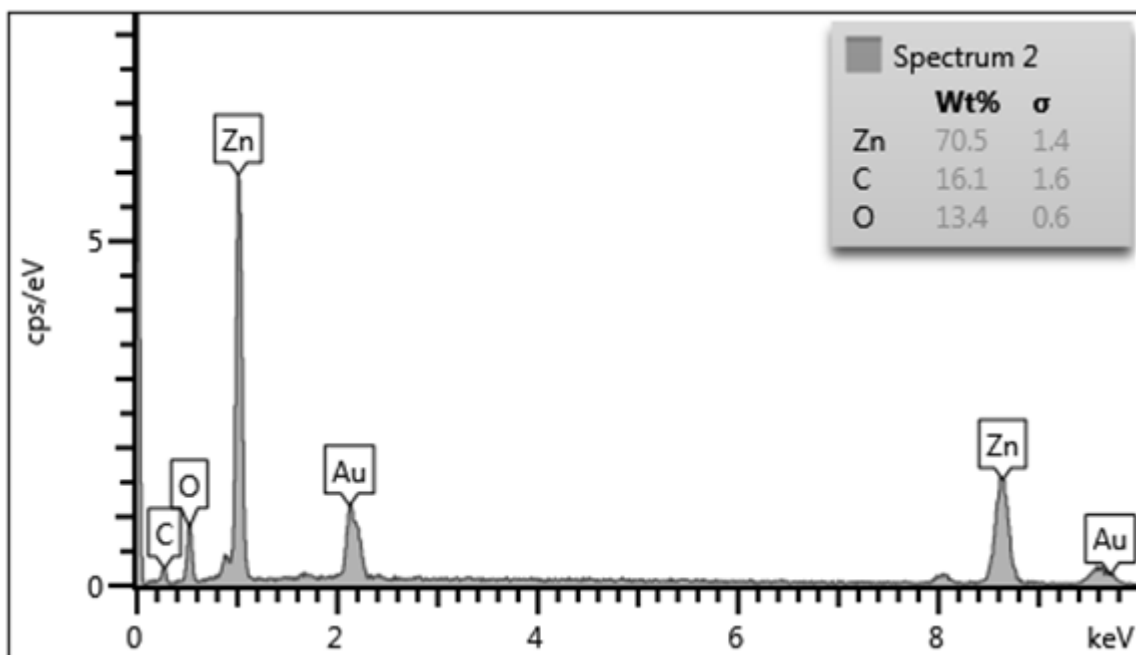


Fig 4 (a) EDX Spectra of undoped ZnO

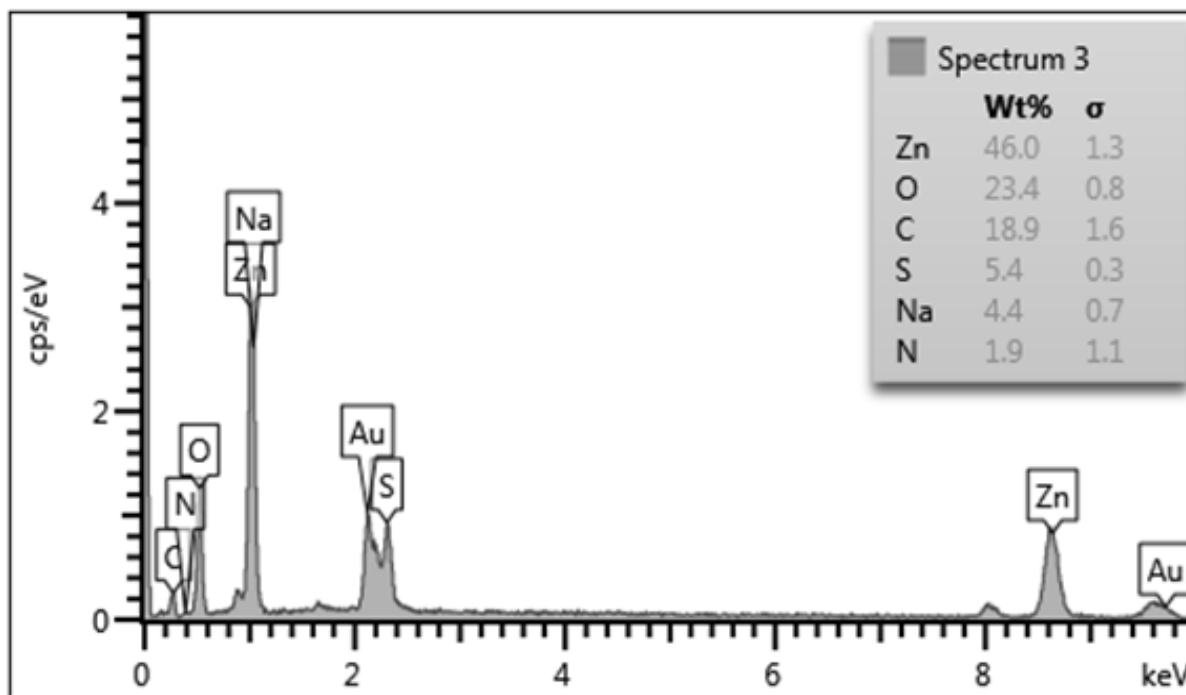


Fig 4 (b) EDX Spectra of N,S-codoped ZnO

The FT-IR spectra is shown in figure 5 above, the main absorption peaks of the sample (N,S-codoped ZnO) were located at 3712-3610 cm^{-1} , 2102-1569 cm^{-1} , and 1540-1167 cm^{-1} . The peaks at 3712-3610 cm^{-1} and 2102-1569 cm^{-1} were assigned to the stretching vibration and bending vibration of surface -OH group. The band at 1018-675 cm^{-1} was assigned to the Zn-O stretching vibration. Zn-O-N and Zn-O-S bonds of the codoped (N, S) sample emerged at 1540 and 1167 cm^{-1} respectively (U.S.LTL ISAT, 2014).

The absence and presence of 1540 and 1167 cm^{-1} absorption bands on the spectrum of figure 4.9 (a) and figure 4.10 (b) respectively have justified the codoping of nitrogen and sulphur on zinc oxide, hence figure 4.10 (a) is an ft-ir spectrum of pure zinc oxide while figure 4.10 (b) shows the N,S-codoped ZnO ft-ir spectrum.

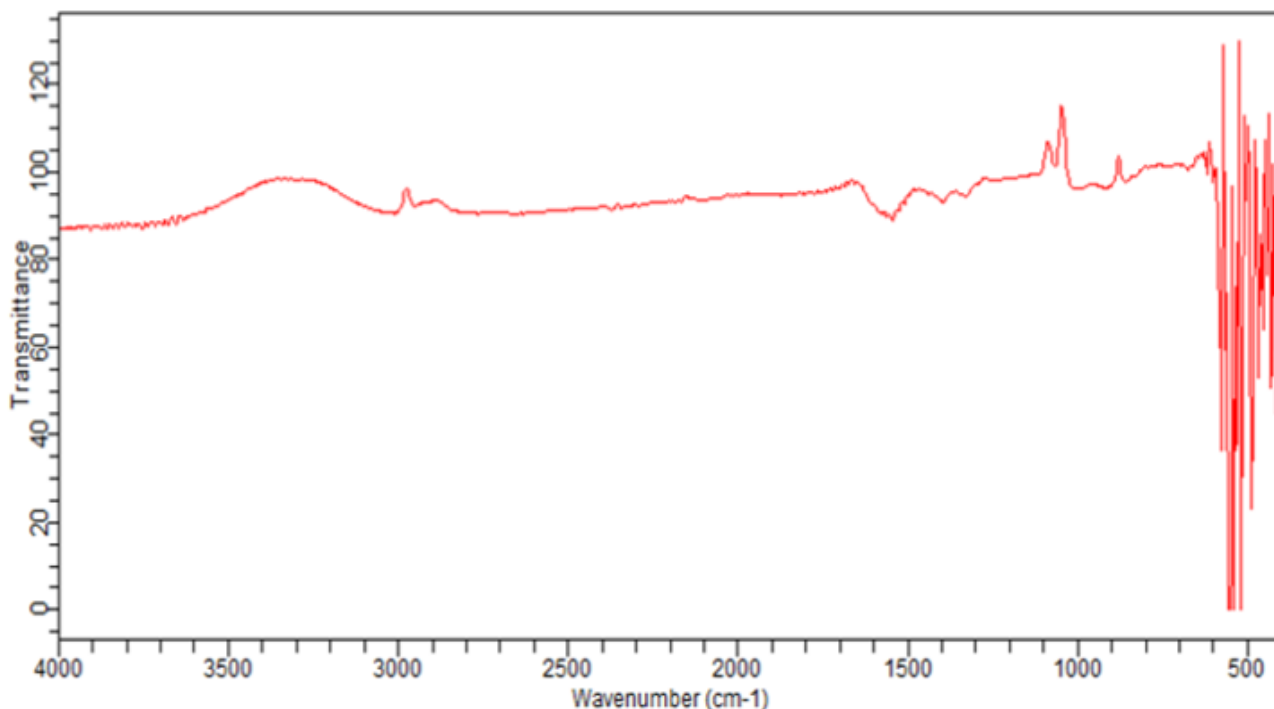


Fig 5 (a) FT-IR spectra of C-doped ZnO

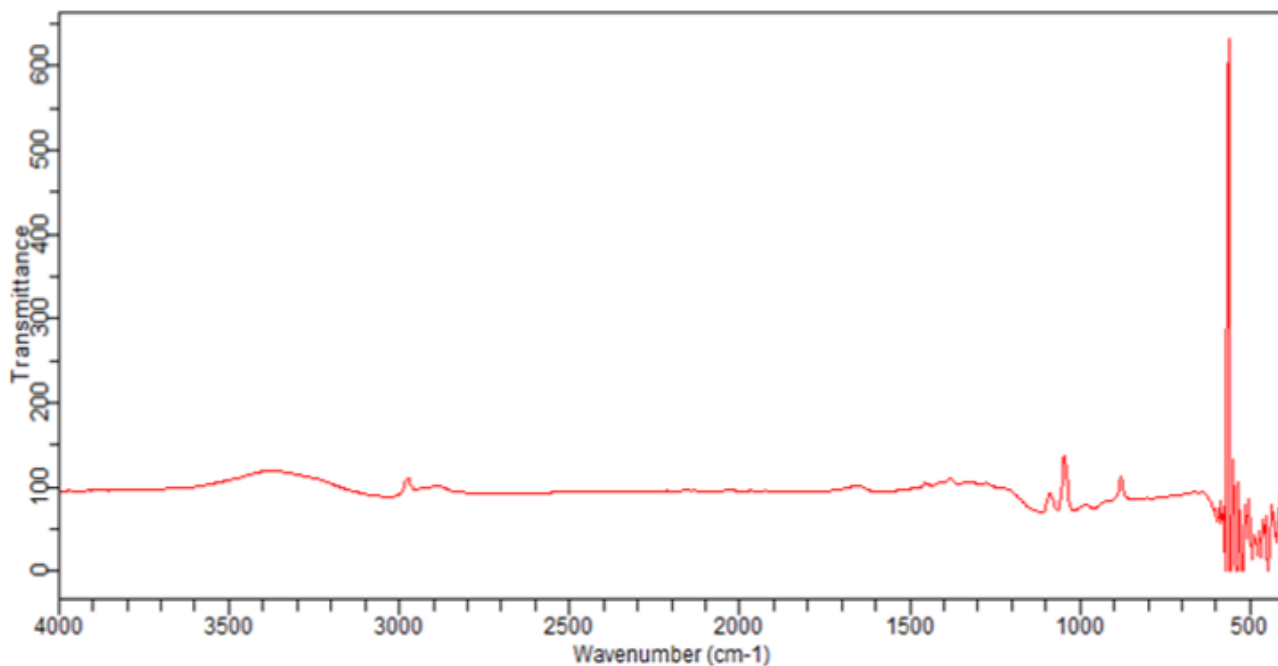


Fig 5 (b) FT-IR Spectra Of C,Nand S tri-dped ZnO

SEM image of undoped ZnO and N, S-codoped ZnO prepared by co-precipitation method was presented in Figure 6 (a) and (b) respectively. It is obvious, that the N,S-codoped ZnO crystal was closely packed together significantly. It can be seen that the size of the microsphere of both the undoped N,S-codoped ZnO is in the range of nanometer. The observation of Figure 6 indicated that the result of SEM is well consistent with the result of XRD. The presence of whitish bigger sulphur crystals are shown on the N,S codoped ZnO surface while the smaller ones are those of nitrogen.

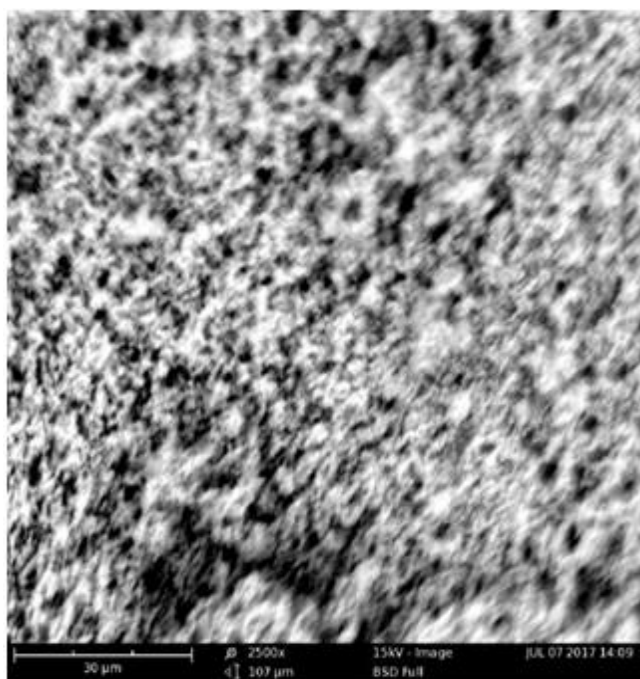


Fig 6 (a) SEM image of undoped ZnO

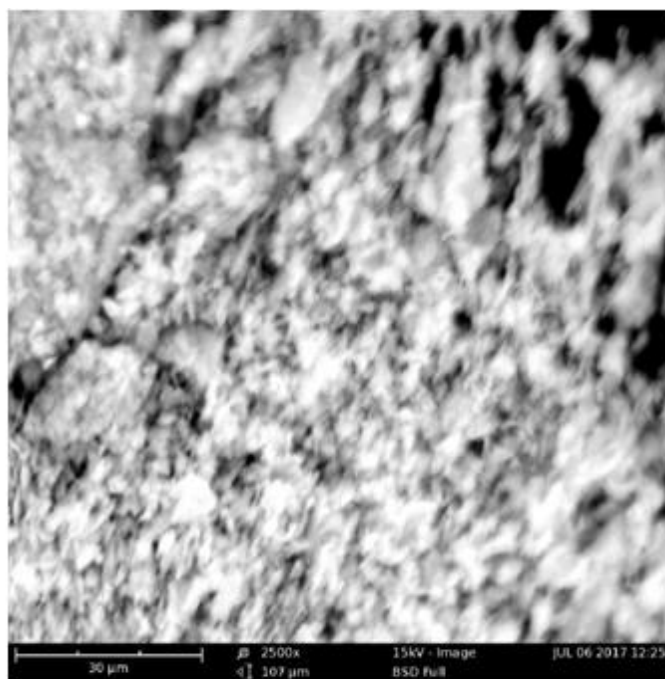


Fig 6 (b) SEM Image of N,S-codoped ZnO

➤ Multivariate optimization

The experimental designed was conducted within the domain shown in Table 1. The input parameters were the initial 4-nitrophenol concentration (*A*), mass of catalyst (*B*) and pH (*C*). The table presents both the actual values and the coded levels (in bracket) of these parameters as used for response surface design. In sum, 20 experiments were performed: 8 factorial, 6 axial and 6 center experiments. The table also shows the experimental responses as well as the predicted responses of the input matrices. The experimental responses were calculated using equation (1). The predicted responses were obtained using DX 6 software.

For prediction of degradation efficiencies, the generic, second order, polynomial regression model was developed.

Table 2 The CCD experimental matrix with response

Run	Variables and Codes			Degradation	
	A	B	C	Experimental (Y _{exp} ,%)	Predicted (Y _{calc} ,%)
1	6(0)	0.15(0)	(-1.682)	51.00	85.00
2	2(-1)	0.2(1)	11(1)	82.23	67.62
3	2(-1)	0.2(1)	11(1)	99.32	92.51
4	2(-1)	0.05(-1)	11(1)	72.12	30.53
5	6(0)	(-1.682)	7(0)	50.60	80.40
6	6(0)	0.075(0)	7(0)	46.72	57.82
7	6(0)	0.015(0)	3(-1)	69.05	92.44
8	10(1)	0.2(1)	3(-1)	34.07	51.14
9	10(1)	0.05(-1)	3(-1)	86.32	94.51
10	2(-1)	0.05(-1)	11(1)	92.08	46.53
11	2(-1)	0.05(-1)	11(1)	85.23	71.00
12	10(1)	0.2(1)	11(1)	64.15	49.64
13	6(0)	0.15(0)	7(0)	60.04	58.04
14	(-1.682)	0.15(0)	7(0)	96.00	73.21
15	6(0)	0.15(0)	7(0)	67.28	58.03
16	6(0)	0.15(0)	7(0)	61.04	58.04
17	6(0)	(1.682)	7(0)	49.26	58.01
18	(1.682)	0.15(0)	7(0)	27.08	58.05
19	6(0)	0.15(0)	(1.68)	59.00	58.42
20	10(1)	0.15(0)	7(0)	48.39	58.10

The closeness of the predicted values to the experimental values is a primary indication of a true model. The optimum degradation efficiency of the photocatalytic reaction (99.3%) was achieved at A= 2Mg/L, B = 0.2 g of N,S-codoped ZnO per 100ml of 4-NP and C = 11. For prediction of degradation efficiencies, the generic, second order, polynomial regression model was developed.

The significance and adequacy of the model was determined by from statistical evidences in the analysis of variance (ANOVA). These evidences include Fischer variation ratio (F- value), probability value (P- value), lack of fit, Coefficient of determination (R²_a), adjusted R-squared (R²_{adj}), predicted R- squared (R²_{pred}) and adequate precision of Predicted Residual Error of Sum of Squares (PRESS) [19]. Most of these parameters are clearly defined in the experimental design parameter texts. PRESS is a signal to noise ratio, which compares the range of the predicted values at the design points to the average prediction error, the ratio greater than 4 indicate the model discriminations [20]. R²_{adj} and R²_{pred} are the measurement of the amount of variation around the mean and the new explained data, respectively.

The very significant is the Fischer test where P value is compared with F value. F value is a statistically valid measure of how well the factors described the variation in the data about its meaning while P value represent the degree of significance of each variable. Mathematically F value is given by the ratio of the mean square due to model variation as shown in the equation below

$$F \text{ value} = \frac{Sr^2}{Se^2}$$

Where Sr² and Se² are mean of the model and residual squared respectively, obtained by dividing the sum of squares of each of the two sources of variation of the model of the error variance by their respective (DF) degrees of freedom [20]. High F value signifies the adequacy of the model. For a variable having a P value smaller than 0.05, responses will be influenced at a confidence level of 0.95.

Table 3 shows the ANOVA result for the quadratic model for the optimised photocatalytic degradation of 4-nitrophenol using N,S-codoped ZnO particles. High F value (2.29) implies the model is significant, there is only a 0.01% chance that a model F value and this could occur due to noise. Values of prob>F less than 0.0500 indicates model terms are significant, in this case A is the significant model term. The lack of fit F value of 0.1375 implies that the lack of fit is not significant relative to the pure error hence, there is high chance that the lack of fit F value, this large could also occur due to noise. However non significant lack of fit is good [21]. The R²_{pred} of 0.3785 is in reasonable agreement with R²_{adj} 0.3799. The adequate precision ratio of 5.578 was obtained which indicate an adequate signal, hence the model can be used to navigate the design space. Therefore the final equation of the model in coded form is given as:

$$Y_{cal} = +58.02 - 14.28A - 6.35B + 4.48C + 4.40A^2 + 0.79B^2 + 2.63C^2 - 4.49AB - 1.97AC + 7.72BC \dots(4.1)$$

Equation (4.1) shows that the ANOVA is utilized to test the significance of each term in regression equation and to fit the resulting regression model. The F-value (2.29) and p-value (0.0375) both agree that the model is significant. The regression model demonstrates a better relationship between independent variables and the response when the R² is close to 1. In this study, the p-values of the major

parameters (A,BandC)influencing the percentage removal of,4-NP are significant ($p < 0.1$). Similarly, the interaction terms (AC and BC) as well as the quadratic terms (A^2 and

C^2) have probabilities less than 0.05, which indicates they significantly contribute to the degradation of 4-NP.

Table 3 Analysis of Variance for the Response Surface Model

Source	Sum of squares	Degree of Freedom(DF)	Mean Sqoare	F Value	Prob> F	
Model	5434.75	9	603.86	2.29	0.1061	Significant
A	2377.78	1	2377.78	9.03	0.0132	
B	470.21	1	470.21	1.79	0.2110	
C	231.75	1	231.75	0.88	0.3703	
A ²	272.64	1	272.64	1.04	0.3329	
B ²	8.88	1	8.88	0.034	0.8580	
C ²	97.58	1	97.58	0.37	0.5562	
AB	125.00	1	125.00	0.47	0.5065	
AC	23.63	1	23.63	0.090	0.7707	
BC	362.86	1	362.86	1.38	0.2676	
Residual	2633.02	10	263.30			
Lack of Fit	2042.97	4	510.74	5.19	0.1375	Not Significant
Pure Error	590.05	6	98.34			
Cor Total	8067.77	19				

The "Model F-value" of 2.29 implies the model is not significant relative to the noise. There is a 10.61 % chance that a "Model F-value" this large could occur due to noise.Values of "Prob > F" less than 0.0500 indicates that model terms are significant. In this case A,B and C are significant model terms. Values greater than 0.1000 indicate the model terms are not significant. If there are many insignificant model terms (not counting those required to support hierarchy), model reduction may be required to improve the model.

The effects of the independent variables and combined effects on the response variable were illustrated by 3D response surface plot (Fig.7). It shows the interaction between the initial concentration of 4-NP and a mass loading of 0.2g/100ml 4-NP solution at constant initial pH (9 units). From the graph, a low initial concentration of 4-NP and a high mass catalyst will produce the highest percentage removal of the pollutant. When the amount of catalyst is high, it is possible to consider the higher pollutant degradation obtained at a 4Mg/L because a lower pollutant concentration allows more UV light penetration, leading to the activation of catalytic sites, which helps to degrade more of the pollutant [22].

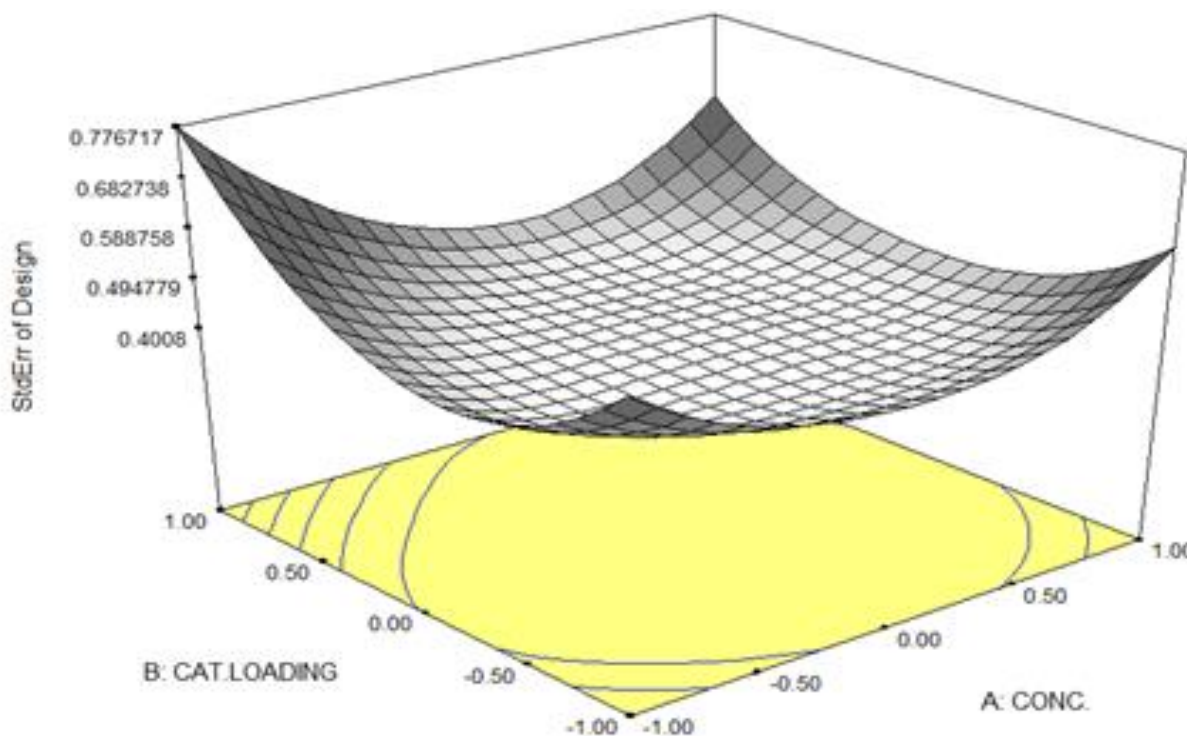


Fig 7 (a) Optimized Effect of Catalyst Vs Concentration

DESIGN-EXPERT Plot

Degradation
X = A: CONC.
Y = C: pH

Actual Factor
B: CAT. = 0.00

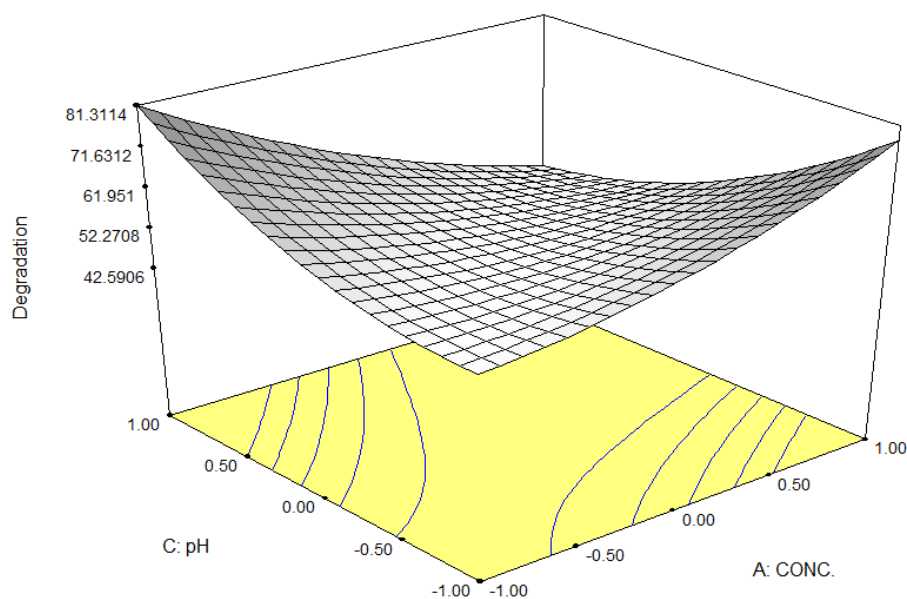


Fig 7 (b) Optimized Effect of pH Vs Concentration

DESIGN-EXPERT Plot

Degradation
X = B: CAT.
Y = C: pH

Actual Factor
A: CONC. = 0.00

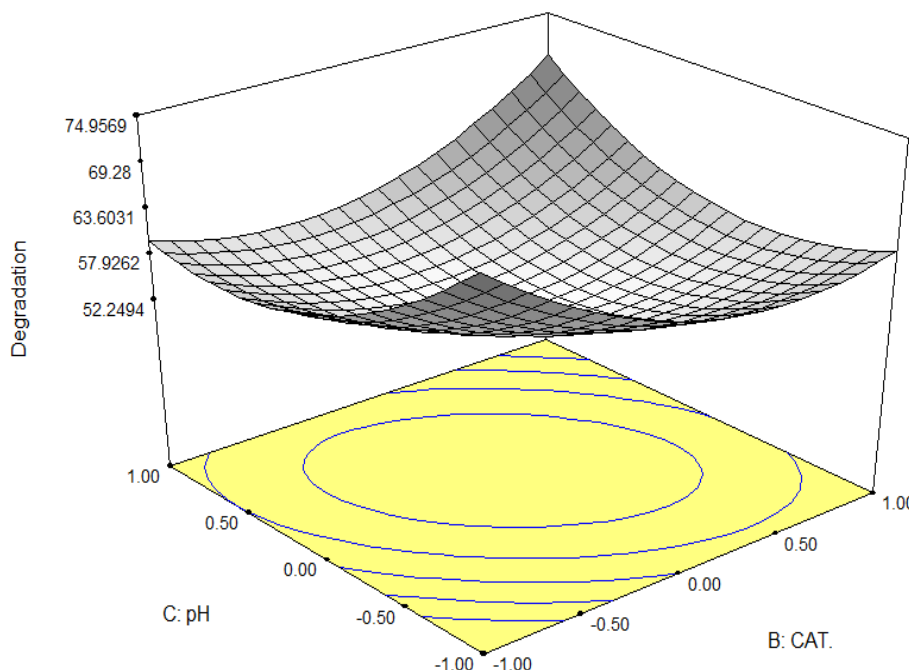
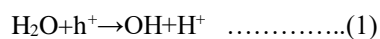


Fig 7 (c) Optimized Effect of pH Vs Catalyst

Figure7 Response surface graphs for the percentage removal of 4-nitrophenol as affected by the initial concentration of 4-NP and catalyst loading (A versus B)

Generally speaking, the degradation of 4-NP is favourable under alkaline conditions (pH 11) but unfavourable under acidic conditions (pH 4). This observation is an indication of the dominance of the oxidative pathway for the generation of reducing species [22] as shown in the following equations:



In the alkaline solution, the OH radical is formed from hydroxide ion



Finally, experiments were performed to validate the statistical model of the study by comparing the experimental and predicted values of 2,4-D removal efficiencies. The experimental data was collected in triplicate under three predictor variables and the degradation efficiency was calculated using equation (2). The experimental and predicted data shown in Table 4, are in good agreement indicating the validity of the analysis.

Table 4 Validation of the Decay Model using New Test Sets

Run	Initial 4-NP concentration (Mg/L)	Catalyst mass (g)	Initial pH	Experimental efficiency	Predicted efficiency
1	2.0	0.15	9.2	97.54 ± 1.43	97.10
2	6.0	0.2	4.6	46.83 ± 1.45	47.20
3	10.0	0.18	5.0	24.57 ± 0.89	24.43

➤ Study of the Effect of Each Photocatalytic Parameters

• Percentage Degradation and Time

The photodegradation of 4-nitrophenol as a function of time is shown in Figure 8 (a) and shows the changes in the visible spectrum of 4-nitrophenol on visible light with N,S-codoped ZnO particles under different irradiation times. For each of the experiment, irrespective of the concentration of pollutant, the % degradation increases with time [23].

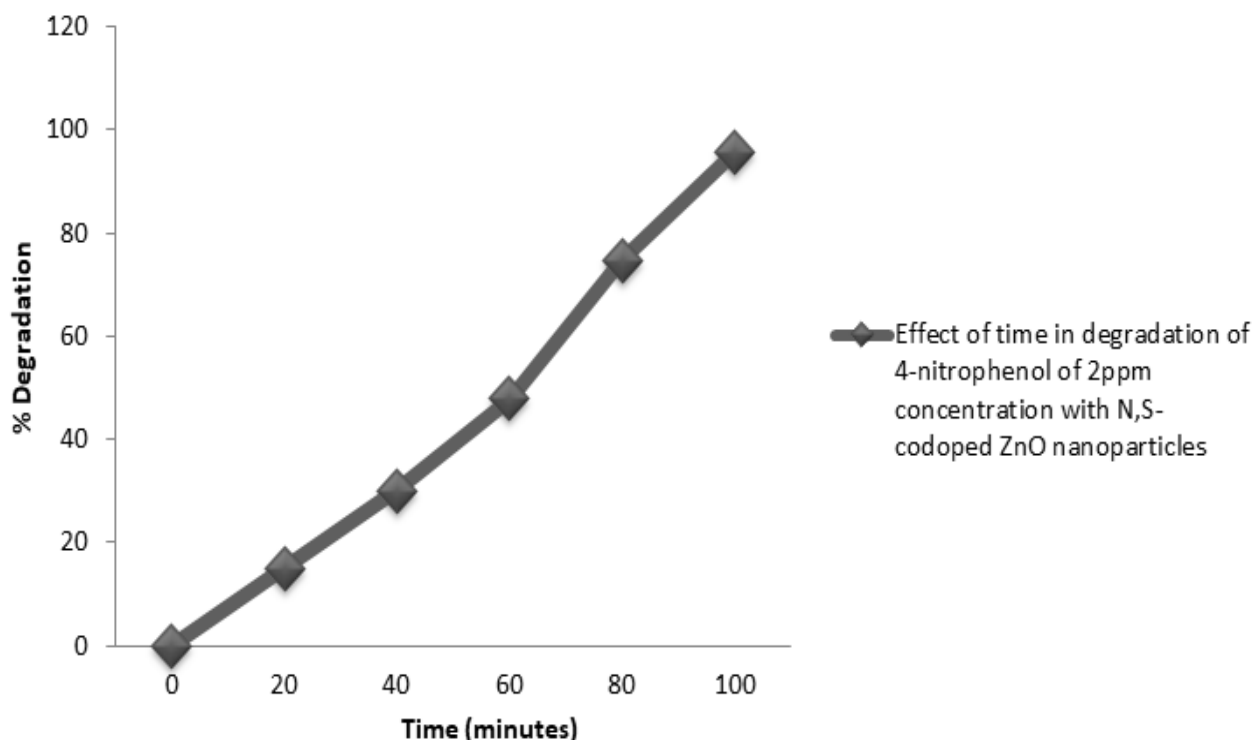


Fig 8 Plot of % Degradation against Time for N,S-codoped ZnO

• Initial Concentration And Percentage Degradation

Figure 9 shows the increase in initial concentration of the pollutant from 2Mg/L to 10Mg/L. There is a decrease in the percentage degradation with increase in concentration of the 4-nitrophenol at fixed pH, catalyst dosage and at room temperature in the same interval of time. This is due to the fact that the higher the concentration of the pollutant, the stronger the bond between the molecules and the more difficult it is for the photocatalyst to break them (Chauhan and Kumar, 2012).

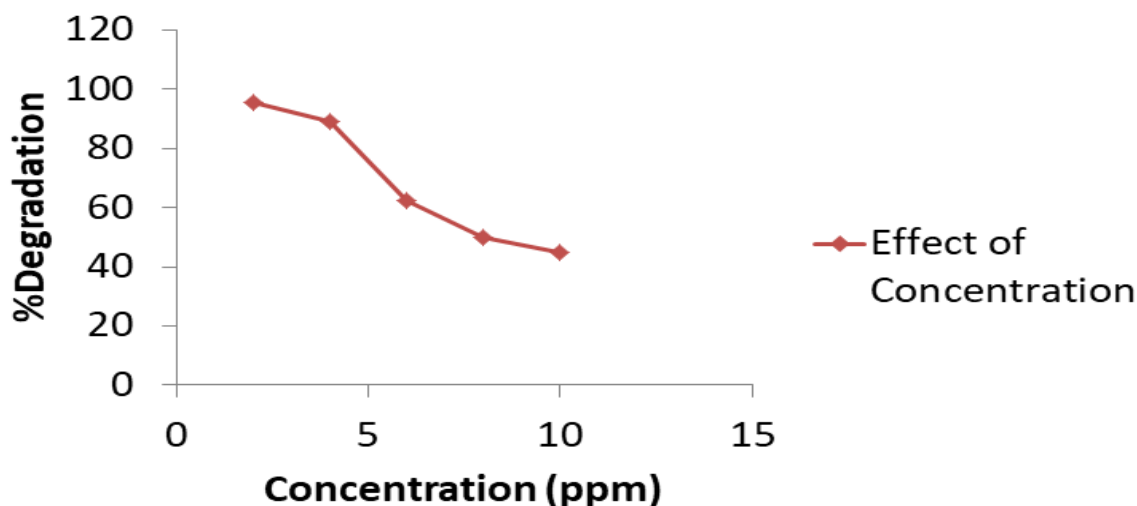


Fig 9 Effect of Increase in Initial Concentration on Degradation of 4-nitrophenol

- *Percentage Degradation and pH*

The most important parameter that influences the photocatalytic degradation is the solution pH. The efficiency of the catalyst is affected by the pH of the solution. The pH of the solution is adjusted before irradiation and it is not controlled during the course of reaction. The effect of varying the pH from 1 to 11 on the degradation of 4-nitrophenol is shown in Fig.10 It was found that the degradation efficiency increases with an increase in pH from 2 to 11. Increase of pH of the 4-nitrophenol solution from 1 to 5 increases the degradation from 29% to 65% at the time of 100 min. A slight increase in the degradation rate was observed for further rise in pH from 5 to 11. Many authors observed similar behavior in their studies [1,22]. At low pH, the N,S co-doped ZnO particles agglomeration reduces the pollutant adsorption as well as photon absorption. The increased efficiency in the alkaline pH range may be explained on the basis of increase in the formation of OH radicals with an increase in pH. In acid and neutral solutions the formation of OH radical can be given by the equation.

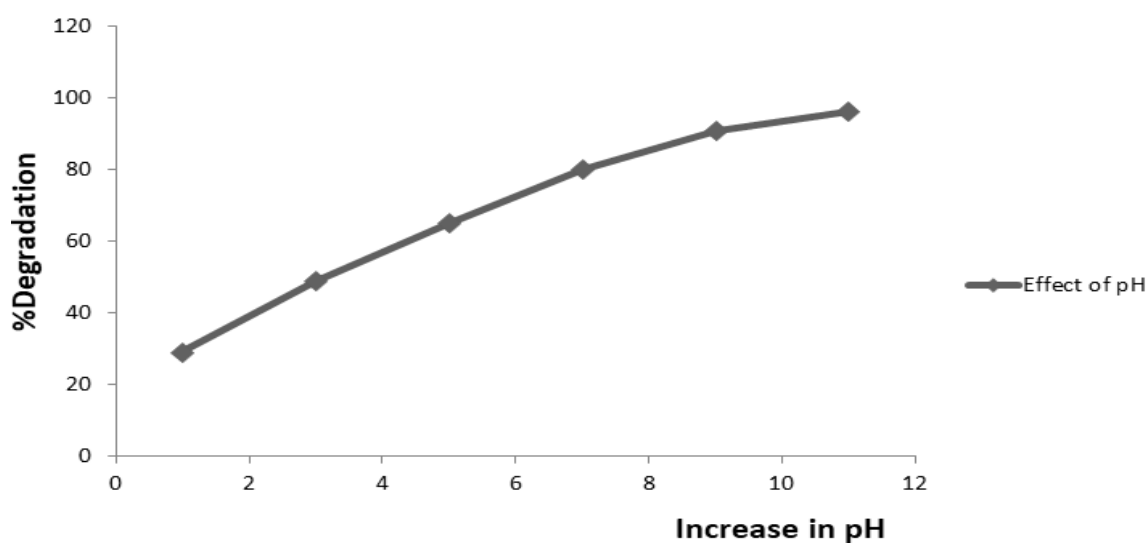


Fig 10 Effect of pH on Degradation of 4-nitrophenol

- *Photocatalyst and Percentage Degradation*

The amount of catalyst is one of the main parameters for the degradation studies. In order to avoid the use of excess catalyst, optimization was carried out by varying the photocatalyst from 0.025g to 0.2g to find out the optimum loading for efficient removal of pollutant. The effect of the amount of catalyst on the photocatalytic degradation of 4-nitrophenol has been carried out in the range of 0.025-0.2g of the catalyst for 50 ml of 4-NP solution. As shown in Fig11, the concentration of the catalyst was increased from 0.025 to 0.1g/50 ml, degradation increases from 25% to 94.9 % at 100min of irradiation time. This is due to an increase in the number of N,S-codoped ZnO particles, which increases the absorption of photons and adsorption of pollutant molecules [23]. Further increase catalyst loading decreases the removal rate. Increase of the catalyst loadings beyond 0.1g/50 ml may cause screening effect, these effects reduce the specific activity of the catalyst [25].

At high loadings of catalyst, particle aggregation may also reduce the catalytic activity [25]. The optimum amount of catalyst loading is found to be 0.1g/50 ml of the degradation of 4-nitrophenol. Hence, 0.1g/50 ml was used as the catalyst dosage for the

photocatalytic reaction. Here it has been observed that the sum of effects of two parameters (pH and catalyst mass) is greater than the individual effect of any one of these parameters. This is known as Synergistic effect.

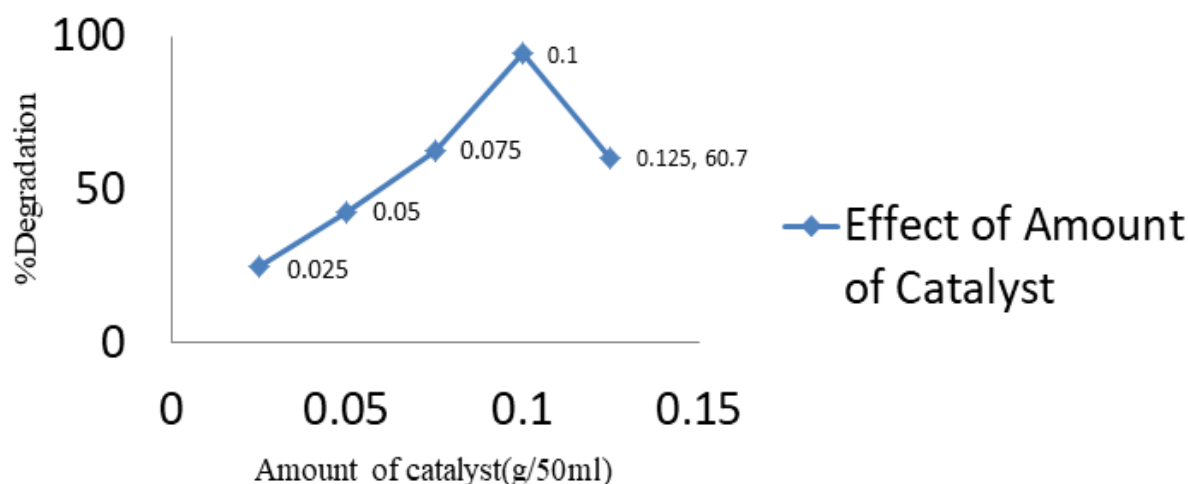


Fig 11 Effect of Increase in Amount of Catalyst on Degradation of 4-nitrophenol

- *Percentage Degradation and Temperature*

There is a significant effect or influence of temperature on the photocatalytic reaction [26]. Figure 12: shows an increase in degradation of 4-nitrophenol of 2Mg/L concentration at fixed pH and catalyst from 293k to 323k, in which degradation was highest at 313-323k (40°C-50°C).

There is a significant decrease in the %degradation at temperature above 323k through which 63% degradation was recorded at 333k.

The fact that when working at a low temperature, the desorption of the products formed reduces the reaction because it is slower than the degradation on the surface and the adsorption of the reactants. At higher temperature, the limiting stage becomes the adsorption of the pollutant molecules on the catalyst [26].

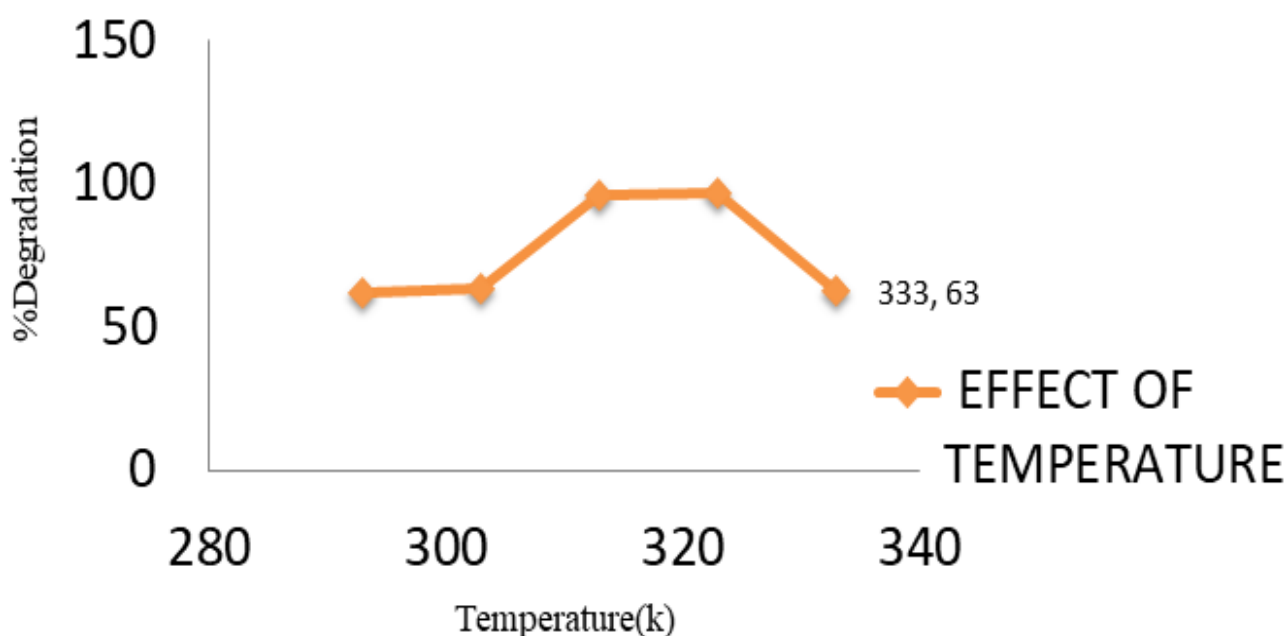


Fig 12 Effect of Temperature on Degradation of 4-nitrophenol

➤ *Comparative Study of Performance between C,N,S-codoped ZnO and C-doped ZnO in Degradation of 4-NP under visible Light*

For each of the experiment, irrespective of the concentration of pollutant, the same effect was observed using undoped ZnO with the visible light irradiation on the pollutant (4-nitrophenol) in which concentration of 2Mg/L has the highest %degradation at optimum pH, catalyst and temperature of 7, 0.2g/100ml and 35°C respectively.

Figure 13 shows that the N,S-codoped ZnO has better photocatalytic activity on 4-nitrophenol than the undoped ZnO under visible light and the same conditions, with 98.7 and 83.3 percentage degradations for codoped and undoped ZnO respectively. The improve in the photocatalytic performance of co-doped sample is due to the reduction in the band gap as a result of the insertion of N and S in ZnO.

Generally doping of semiconductor reduces the band gap energy and increases the spectral response of the semiconductor to visible light[27].

The %degradation of 4-nitrophenol of 2Mg/L concentration with N,S,-codoped ZnO was found to be higher than undoped ZnO under the same conditions. This has justified the doping turning of the semiconductor photocatalyst (ZnO), hence improved photocatalytic activity from 83% to 98.7% degradations for undoped and N,S-codoped ZnO respectively have been achieved for 100minutes irradiation time.

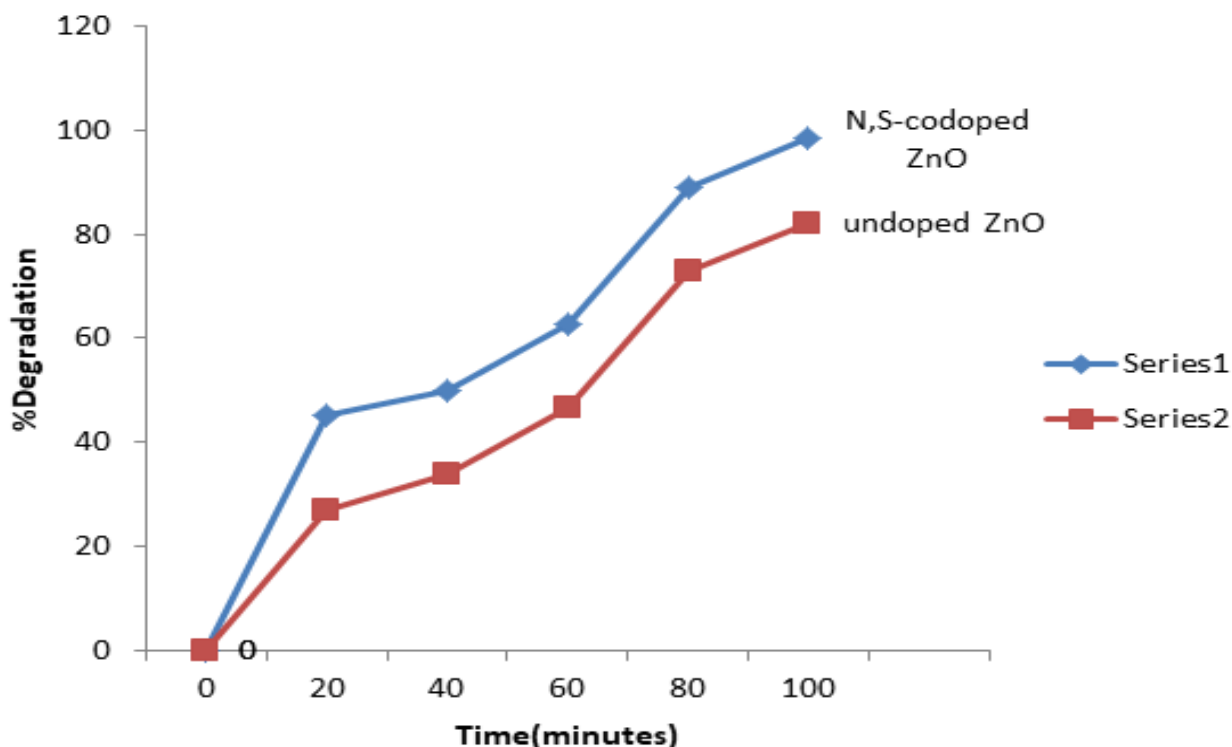


Fig 13 Study of Photocatalytic Performance of N,S-codoped and undoped ZnO

IV. CONCLUSION

Doped ZnO semiconductor material efficient for photocatalytic removal of organic pollutant have been successfully synthesized through co-precipitation method as justified by the characterization results. In this method nitrogen and sulfur codoping by using a single source (ammonium sulfate) as the modification agent of zinc oxide and zinc acetate dihydrate as the precursor. photocatalytic activity of the N,S-codoped ZnO have been investigated on degradation of 4-Nitrophenol, and was compared with that of undoped ZnO, the results indicated that photocatalytic activity of ZnO (N,S-codoped) on 4-nitrophenol under visible light irradiation is about 99.3% for 0.2g/100ml in 100minutes, which is greater than that of undoped ZnO found to be 82% under the same conditions. However, the band gap energy of the catalysts was red-shifted, thus reassuring the photoresponse of the doped semiconducting material all over the UV region. The catalyst's activity over many cycles of 4-NP photodegradation as in the design shows remarkable applicability in environmental treatment technologies. The degradation was more favourable in

alkaline medium, suggesting the possibility of the reduction pathway.

Hence N,S-codoped ZnO synthesized via co-precipitation can be utilized for clean-up of environment affected by 4-nitrophenol following the above method.

REFERENCES

- [1]. Chiara Gionco, Debora Fabbri, Paola Calza, and Maria Cristina Paganini.(2016). Synthesis, Characterization, and Photocatalytic Tests of N-Doped Zinc Oxide: A New Interesting Photocatalyst, Dipartimento di Chimica, Università di Torino, Via P. Giuria 7, 10125 Torino, Italy.
- [2]. Valencia, S., Marin, J. M., & Restrepo, G. (2010). Study of the Bandgap of Synthesized Zinc oxide Nanoparticles Using the Sol-Gel Method and a Hydrothermal. The Open Materials Science Journal, 4(2), 9–14.

- [3]. Khan et al.,(2015). Nanomaterial for Photocatalysis and their Application in Environmental clean-up. Centre for Nano Sciences, Central of Gujarat, Gandhinagar, India 382 030 2School of Environment and Sustainable Development, Central of Gujarat, Gandhinagar, India 382 030.
- [4]. Ahmed, S., Rasul, M.G., Martens, W.N., Brown, R.J., & Hashib, M.A. (2010) Heterogeneous photocatalytic degradation of phenols in wastewater : a review on current status and developments. *Desalination*, 261(1-2), pp. 3-18.
- [5]. Chen L.C., Huang C.M., Hsiao M.C., Tsai M-R. *Chem Eng J*, (2010), 'Photocatalytic degradation of chloro phenols on N-doped ZnO under UV light, 34(11) 165- 482.
- [6]. Ravelli, D., Dondi, D., Fagnoni, M. & Albinì, A. (2013). Photocatalysis. A multi-faceted concept for green chemistry. *Chemical Society Reviews*, 38(7), 543-654.
- [7]. Gaya U I. Heterogeneous photocatalysis using inorganic semiconductor solids. Dordrecht: Springer, 2014 Steinfeld, A. (2016). Solar hydrogen production via a two- step water-splitting thermochemical cycle based on Zn/ZnO redox reactions. *International Journal of Hydrogen Energy*, 27(6), 611–619.
- [8]. Mina Zare, Keerthiraj N. and Xian Zhang (2019) “Novel green biomimetic approach for synthesis of Ag-doped ZnO for removal of substituted phenols by solar photocatalysis, *Journal of chemical engineering* 24(2) 561-584.
- [9]. Hazardous substances data bank (HSDB) (2016), 'Current research on the trend of organic pollutant in the environment, 12(9) 251-258.
- [10]. Khan, S. Fulekar, M.H and Bhuwana S.(2015), Nanomaterials for photocatalysis and their application in Environmental Clean-up. *International journal of current research*, 6(7): S23-123.
- [11]. Xiao-Hong Zou, Si-Wei Zhao, Ji-Guo Zhang, H. Liang and Qing Jiang P. (2019) “Preparation of ternary Ag-ZnO/cellulose and its enhanced photocatalytic degradation property on phenol and benzene in COCs, *Open chemistry* 17(5) 265-309.
- [12]. Lathasree, S., Rao A.N., Siva Sankar, B., Sadasivam V. and Rengaraj, K. (2014) Heterogeneous photocatalytic mineralization of phenols in aqueous solutions. *Journal of Molecular Catalysis A: Chemical* 223, 101-105.
- [13]. Martens, W.N. Brown, R.J. & Hashib, M.A.(2017) 'Heterogeneous photocatalytic degradation of substituted phenol in wastewater, *Desalination*, 141(3-7) 6-32.
- [14]. Pacchioni K. and Valentin C. (2015) Synthesis and characterization of tridoped ZnO for photocatalytic degradation of phenols, *Journal of chemical Research*, 96(5) 264-341.
- [15]. Rahimi R., Samaneh Safawu M. and Mahboubeh Rabbani (2016) “Photocatalytic degradation of 4-nitrophenol in aqueous N,S-codoped TiO₂ suspension, *Tahram*, (17) 16846-13114.
- [16]. Dewidar H., S. A. Nosier and Ahmad EL-Shazly (2017) “Photocatalytic degradation of 4-nitrophenol solution using S-doped ZnO and UV light, *Journal of chemical health and safety* 25(1) 291-306.
- [17]. Rao K., Lavedrine B., P., and J. A.W, (2015) “Photocatalytic removal of phenols in water using C-doped ZnO , *journal of photochemistry and biochemistry*, (33) 65-157.
- [18]. Behzad S., Farzaneh Farahani, Shadi K. Afshin Maleki, M. Pordel and Y. Zandsalimi (2019) “Application of Cd-doped ZnO for solar photocatalytic degradation of phenol, *Water science and technology* 79(2): 375-387.
- [19]. Serponse N. and Alberto E.C. (2016) 'Photocatalytic degradation of some selected dyes on S-doped ZnO under UV, *Journal of Physical Chemistry*, 107(6), 217-309.
- [20]. Zhenghui Lill, Wenyu Xie, Dehao Li. Yangpeng, Zeshig Li and Shusi Liu (2016) “Biodegradation of phenol by bacteria strain *Acinetobacter calcoaceticus* PA Isolated from phenolic waste water, *International Journal of Environmental Research and Public Health* 13(3): 300.
- [21]. Maria E. M., Luis Enrique Norena, Francisco T., Jose G. H. and Liqun Ye (2018) “Ono-pot synthesis of Ru-Doped ZnO for photodegradation OF 4-Chlorophenol , *International Journal of photoenergy* 36(3) 361-401 United state Environmental Protection Agency (2008).
- [22]. Hazardous substances data bank latest update, 2016.
- [23]. Andre, A., Valentin N.P. and Nick, S. (2014) 'Degradation of organic pollutants in waste water' *IUPAC* 96(2) 721-810.
- [24]. Abdollahi, Y., Abdullah, A. H., Zainal, Z., & Yusof, N. A. (2011). Photocatalytic degradation of p-Cresol by zinc oxide under UV irradiation. *International journal of molecular sciences*, 13(1), 302-315.
- [25]. Gaya U I, Abdullah A H, Zainal Z, Hussein M Z. *J Hazard Mater*, 2009, 168: 57.
- [26]. Chen L-C, Huang C-M, Hsiao M-C, Tsai M-R. *Chem Eng J*, 2010, 165: 482.
- [27]. Kimura, S., Kodama, S., & Sekiguchi, H. (2013). Development of photocatalytic reactor having light source inside by electrical discharge, (August), 4–7.
- [28]. Abdollahi, Y., Zakaria, A., Abdullah, A. H., Fard Masoumi, H. R., Jahangirian, H., Shameli, K., ... Abdollahi, T. (2012). Semi-empirical study of ortho-cresol photo degradation in manganese-doped zinc oxide nanoparticles suspensions. *Chemistry Central Journal*, 6(9), 88.
- [29]. Hoffmann M R, Martin S T, Choi W, Bahnemann D W. *Chem Rev*, 1995, 95: 69.
- [30]. Abdollahi, Y., Abdullah, A. H., Gaya, U. I., Zainal, Z., and Yusof, N. A. (2012). Enhanced photodegradation of o-cresol in aqueous Mn(1%)-doped ZnO suspensions. *Environmental Technology*, 33(10), 1183-1189.

- [31]. Rahmatollah Rahimi, Mahboubeh Rabbani, Samaneh Safalou Moghaddam. (2012). Photocatalytic degradation of 4-nitrophenol using N,S-codoped TiO₂ nanoparticles, Carp O, Huisman C L, Reller A. *Prog Solid State Chem*, 2004, 32: 33.
- [32]. Afini RAZANI, Abdul Halim ABDULLAH, Anwar FITRIANTO, Nor Azah YUSOF and Umar Ibrahim GAYA (2015) “Optimized photocatalytic degradation of 2,4- dichlorophenoxyacetic acid over nanocrystalline iron-doped TiO₂ photocatalyst” 11
- [33]. Abdollahi, Y., Zakaria, A., Abdullah, A. H., Fard Masoumi, H. R., Jahangirian, H., Shameli, K., Abdollahi, T. (2012). Semi-empirical study of *ortho*-cresol photo degradation in manganese-doped zinc oxide nanoparticles suspensions. *Chemistry Central Journal*, 6(9), 88.
- [34]. Chen, W., Qi, D., Gao, X., Thye, A. and Wee, S. (2009). ‘Transfer doping of semiconductors, *Progress in Surface Science*, 84(9): 279–321.
- [35]. Abdollahi, Y., Zakaria, A., Sairi, N. A., Amin Matori, K., Fard Masoumi, H. R., Sadrolhosseini, A. R., & Jahangirian, H. (2014). Artificial Neural Network Modelling of Photodegradation in Suspension of Manganese Doped Zinc Oxide Nanoparticles under Visible-Light Irradiation. *The Scientific World Journal*, 72(6), 101.
- [36]. Shchukin, D. G., & Sviridov, D. V. (2006). Photocatalytic processes in spatially confined micro- and nanoreactors. *Journal of Photochemistry and Photobiology C: Photochemistry Reviews*, 7(1), 23–39.
- [37]. Rivera-Utrilla J, Sánchez-Polo M, Abdel daiem M M, Ocampo-Pérez R. (2012) Applied photocatalytic degradation methyl orange under uv light, 591(5), 100-126.
- [38]. Chauhan, R. and Kumar, A. (2012). Photocatalytic studies of silver doped ZnO nanoparticles synthesized by chemical precipitation method, *Chemical Science* 6(7) 546–553.